Journal of Applied Electrochemistry **32**: 1–10, 2002.

Electrodeionisation 3: The removal of nickel ions from dilute solutions

P.B. SPOOR[1]*, L. KOENE[1], W.R. TER VEEN[2] and L.J.J. JANSSEN[1]
[1]*Department of Chemical Engineering, Eindhoven University of Technology, Laboratory of Process Development, P.O. Box 513, 5600 MB Eindhoven, The Netherlands*
[2]*TNO Institute of Environmental Sciences, Energy Research and Process Innovation, Laan van Westenenk 501, P.O. Box 342, 7300 AH Apeldoorn, The Netherlands*
*(*author for correspondence, e-mail: p.b.spoor@tue.nl)*

Received 23 April 2001; accepted in revised form 18 October 2001

Key words: continuous deionisation, electrodialysis, ion exchange, nickel ions

Abstract

The removal of nickel ions from dilute solutions using a process that combines an ion-exchange bed with electrodialysis has been studied. The main aspects include: the concentration of nickel ions in the diluate, the voltage over the cell and the current density distribution along the ion-exchange bed. The current density distribution provides insight into the state of the bed as it is simultaneously loaded with Ni^{2+} and regenerated with an electric potential difference applied perpendicular to it. A simple model is used to describe the state of the bed and the quantity of nickel removed from it as a function of time. Under specific conditions the precipitation of metal hydroxides is observed in the compartment containing the ion-exchange bed. The results show that hydroxide precipitation is related to the nickel concentration in solution and the electric potential gradient across the bed.

List of symbols

A_b	area of the bed perpendicular to feed flow (m^2)
c	concentration of species (mol m^{-3})
D	diffusion coefficient (m^2 s^{-1})
d	species deposited on cathode
d_{bed}	distance between the two ion-exchange membranes (m)
E_i	potential difference over component i (V)
F	Faraday constant (C mol^{-1})
grad φ	potential gradient (V m^{-1})
K_a	equilibrium constant
k_m	transport coefficient to cathode membrane (m s^{-1})
l	characteristic length (m)
N	flux of species to cathode compartment (mol m^{-2} s^{-1})
n	quantity of species (mole)
Q_s	volumetric flow rate of solution (m^3 s^{-1})
R	resistance (Ω), gas constant (VC mol^{-1} K^{-1})
Re	Reynolds number
Sc	Schmidt number
Sh	Sherwood number
T	temperature (K)
t	time (s)
t_{cap}	time at which a bed segment was converted to the nickel form (s)
V_i	volume of bed in i form (m^3)
w	width of ion exchange bed perpendicular to the potential gradient (m)
z	axial position in ion-exchange bed (m), ionic valence (−)
ΔE_i	electric potential difference over component i (V)
ε	void fraction of ion-exchange bed
v	linear solution flow rate (m s^{-1})
υ	kinematic viscosity (m^2 s^{-1})

Subscripts

a	anode compartment, anolyte
anode	platinum anode
bed	ion exchange bed
c	centre compartment
d	deposit on cathode
cathode	platinum cathode
cell	entire cell including electrodes, electrolytes, membranes and ion-exchange bed
cap	capacity
e	effluent solution
eff	effective or apparent parameter
f	feed
k	cathode compartment, catholyte
i	ion
lim	limiting
R	resin phase
r	quantity removed from model feed solution
S	solution phase
S–R	combination of solution and resin phase
seg	segment

Symbols with over bars (e.g. $\bar{c}_1$) indicate values within the ion-exchanger.

1. Introduction

The electrodeionisation process is a means by which the continuous and cost-effective recovery of heavy metals from dilute solutions may be realised. By placing an ion-exchange resin in the diluate compartment of an electrodialysis cell, the technique combines the added selectivity and conductivity provided by the ion-exchange column with the advantages of electrodialysis. Several factors regarding the removal of sorbed nickel ions from a bed of ion-exchange particles have been studied in previous papers [1–3]. These include the effect of Ni^{2+} concentration in the particles, magnitude of the applied cell voltage, bed width, acid concentration of the electrolytes as well as other factors that were observed to affect the steady state of the process at longer periods of operation.

The aim of the present work is to study the effects of nickel feed concentration, and to examine the current density distribution along the cell as it is simultaneously fed with a dilute nickel solution and regenerated with a constant potential difference. Two different ion-exchange materials have been used, one with a flexible gel matrix and one with a rigid macro-reticular matrix. The rigid macro-reticular *Amberlyst* 15 ion exchange resin was used in the study incorporating various nickel concentration in the feed solution. Its high degree of cross-linking (approximately 20%) renders it very stable and, consequently, the size of the 'macro' pores are fixed. The second type, the *Dowex 50WX*-2 ion-exchanger, is a 2% cross-linked gel that swells and creates space between the polystyrene chains through which ions can migrate [4]. This resin was used in the study of the current density distribution over a 0.5 m tall bed during the electrodeionisation process. The two resins differ greatly in their electrical conductivity and physical stability; it was found that the highly flexible *Dowex 50WX*-2 ion-exchange resin has a much higher conductivity but lower stability than *Amberlyst 15* [1, 2].

2. Experimental

2.1. *Mass transfer during electrodialysis*

The electrodialysis experiments were carried out using a cell consisting of three compartments (anode, cathode and centre) divided by an anion-selective membrane on the anode side and a cation-selective membrane on the cathode side of the centre compartment. The effective area of the cell (i.e. membrane and electrode area) was 0.001 m^2 (0.100 m in height). The centre and outer compartments had widths of 0.015 and 0.0050 m respectively.

Each experiment employed one of the following exchange resins: (a) *Amberlyst 15* containing sorbed Ni^{2+} and Na^+, (b) *Amberlyst 15* containing sorbed H^+, (c) *Dowex 50WX-2* containing sorbed Ni^{2+}. Exchanger-a was prepared in batch by equilibrating the resin, originally in the sodium form, with two bed-volumes of 215 mol m^{-3} $NiSO_4$ solution over a period of 20 days. The resin was then washed with deionised water and later stored in a beaker containing two bed-volumes of deionised water. The retinate was then analysed for nickel content. Exchanger-b was prepared by placing a quantity of the resin in a column and, to ensure its hydrogen form, it was subsequently regenerated with 2 M sulphuric acid. It was then washed with deionised water until the retinate was neutral. The preparation of exchanger-c was performed in batch and is described in Ref. [2].

The effects of the $NiSO_4$ concentration in the feed solution (1.3, 2.8, 4.7, 5.7 and 8.2×10^{-4} M) on the mass transfer of Ni^{2+} were studied using exchanger-a. Exchanger-a was used to ascertain the origin of the ions present in the effluent, i.e. Na^+ from the exchanger and H^+ from the outer compartments [1]. The results were then compared to experiments using *Amberlyst 15* in the hydrogen form (exchanger-b) and the *Dowex* resin in the nickel form (exchanger-c). These latter experiments were carried out with a 0.001 M $NiSO_4$ feed solution.

All experiments were performed by placing an aliquot of the resin in the centre compartment of the cell. A solution containing a pre-determined concentration of $NiSO_4$ at a pH of 5.70 was introduced to the centre compartment at a flow rate of 25 cm^3 min^{-1}, while sulphuric acid solutions with concentrations of 0.1 M were circulated through the outer compartments. During each run a constant cell voltage of 30 V was applied and the following characteristics were monitored:

- current (hourly)
- centre compartment solution conductivity and pH at the outlet
- temperature of all three solutions

Samples of the catholyte (1 cm^3) and effluent (2 cm^3) were taken on an hourly basis and analysed for Ni^{2+}. Effluent samples from a selection of the experiments were also analysed for Ni^{2+} and Na^+.

Nickel and sodium concentrations were determined using a Perkin-Elmer 3030 atomic absorption system. The absorption was linear between 0 and 1 ppm for sodium and 0 and 2 ppm for nickel, while solutions found outside these ranges were diluted with deionised water. The lower detection limit for nickel was approximately 4.3×10^{-3} and 2.0×10^{-4} ppm for sodium. All analyses were performed using an air/acetylene flame and a detection wavelength of 232.0 nm for nickel and 589.0 nm for sodium.

2.2. *Current distribution along a tall vertical cell with segmented electrodes*

The cell used in this series of experiments contained segmented electrodes. It is depicted in Figure 1. The effective height of the cell was 0.50 m and it consisted of

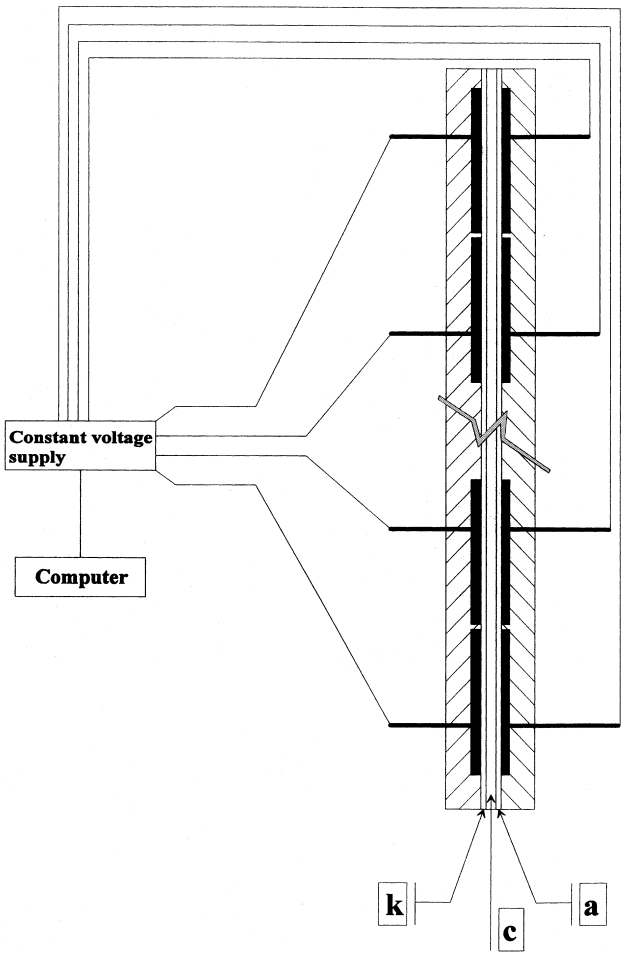

Fig. 1. Section of the segmented electrode cell depicting the anode (a), cathode (k), and centre (c) compartments.

three compartments (anode, cathode and centre) separated by two *Nafion 117* cation selective membranes. The outer compartments, which housed the electrodes, were 0.01 m wide and 0.005 m thick while the centre compartment had horizontal dimensions of 0.01 by 0.01 m respectively. Each electrode comprised 20 flat platinum segments. Each segment was 0.0240 m in height, 0.010 m in width and separated by a distance of 0.0010 m. The segments in the electrode compartments were aligned directly opposite one another and each of the 20 pairs were connected to a separate channel of a power supply [5].

The anode and cathode compartments were connected to separate flow circuits, each containing a 1 M H_2SO_4 solution, while a bed of *Dowex 50WX-2* ion-exchange particles in the hydrogen form was placed in the centre compartment. A 0.001 M $NiSO_4$ model solution was then treated by passing it through the centre compartment of the cell at a flow rate of 33 cm^3 min^{-1}. All solutions were kept at a constant temperature of 298 K. During electrodialysis, the current density across each electrode segment pair was recorded every 15 min and 1.5 cm^3 catholyte samples were taken periodically and analysed for Ni^{2+} content. This procedure was carried out for cell voltages of 5, 10 and 15 V.

2.3. *Apparent nickel capacity of Dowex 50WX-2*

Due to the large degree of swelling of the 2% cross-linked resin, the apparent concentration of fixed sites in its Ni^{2+} form distinctively varies from that of the H^+ form, and hence that given by the supplier (600 mol m^{-3}). To determine the apparent nickel capacity of the ion-exchange bed, a quantity of *Dowex 50WX-2* resin in the hydrogen form was placed in a calibrated column with a cross sectional area of 1 cm^2. The settled volume of the resin was 19.1 cm^3. Top down flow of deionised water was then induced by a suction pump at a pressure of 0.6 bar (equal to the initial pressure across the 70 cm tall cell filled with the nickel form of a 50 cm tall *Dowex 50WX-2* bed). The bed volume was then re-measured and was found to have decreased by 7% to 17.8 cm^3. A 0.1 M $NiSO_4$ solution was then trickled through the column until the retinate had the same composition as the $NiSO_4$ feed (at this point the bed had been fully converted to the nickel form; it was determined by measurement of the retinate pH). The ion exchange bed, now in the nickel form, was then washed with five bed-volumes deionised water (to remove $NiSO_4$ from the interstitial solution), and the retinate analysed for nickel content by AAS. The quantity of nickel sorbed by the bed was determined by calculating the difference between the quantity of nickel fed to the bed and the quantity remaining in the retinate. Top down flow of deionised water was again stimulated by a suction pump at a pressure of 0.6 bar to determine the volume of the bed under operating conditions. The volume of the resin in the nickel form was found to have decreased by approximately 40% to 10.8 cm^3 upon conversion from the hydrogen to nickel form and the effective nickel capacity of the contracted *Dowex 50WX-2* was found to be 534 mol m^{-3}.

3. Results

3.1. *Mass transfer during electrodialysis, Amberlyst 15*

The effect of nickel concentration in the feed solution, $c_{Ni,f}$, on the migration rate of nickel in a bed of *Amberlyst 15* particles loaded with nickel and sodium was studied [effective nickel content: 334 mol m^{-3} wet settled bed (40%), effective sodium content 1050 mol m^{-3} (60%)]. During the course of the experiment a gradual increase in current density, from approximately 5 to 14 mA cm^{-2}, and the formation of a greenish precipitate on the ion-exchange particles at the inlet side of the cell were observed. The quantity of nickel transported from the centre compartment, through the cation-selective membrane and into the cathode compartment is presented in Figure 2 for the 1.3, 2.8, 5.7 and 8.2×10^{-4} M $NiSO_4$ experiments. The rate of nickel transport increased with increasing $c_{Ni,f}$ and decreased with increasing time of electrodialysis.

The various contributions to the mass balance of the system is depicted in Figure 3 as a function of the nickel

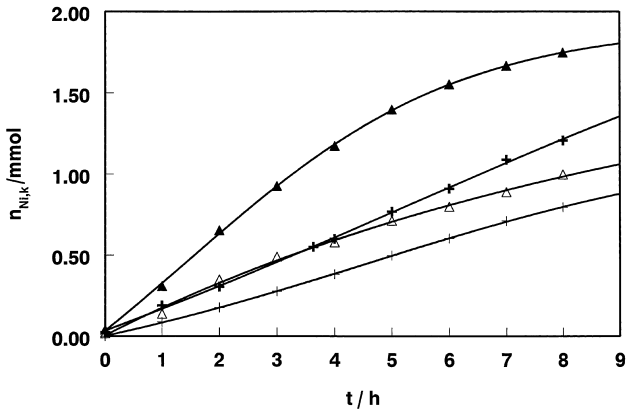

Fig. 2. The amount of nickel ions in the catholyte as a function of time for the series of experiments in which a bed of *Amberlyst 15* particles loaded with Ni^{2+} and Na^{+} was used and the nickel concentration in the feed solution, $c_{Ni,f}$, was varied. A constant cell voltage of 30 V was applied for all experiments and feed solution flow rate was 25 cm^3 min^{-1}. $c_{Ni,f}$: (+) 1.3×10^{-4}; (△) 2.8×10^{-4}; (+) 5.7×10^{-4}; (▲) 8.2×10^{-4} M $NiSO_4$.

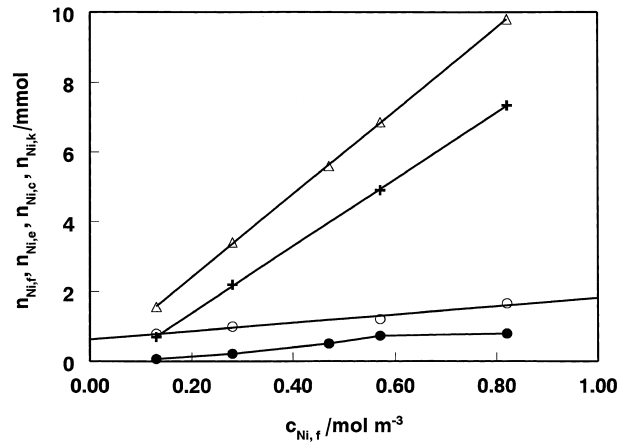

Fig. 3. The total quantity of nickel transported into the cathode compartment, $n_{Ni,k}$ at a cell voltage of 30 V (○), the total quantity of nickel fed to the cell, $n_{Ni,f}$ (△), the total quantity of nickel remaining in the centre compartment, $n_{Ni,c}$ (+), and the total quantity remaining in the effluent, $n_{Ni,e}$ (●) after 8 h electrodialysis as functions of the nickel concentration in the feed solution.

feed concentration, $c_{Ni,f}$. These include the amount of Ni^{2+} transported to the cathode compartment, $n_{Ni,k}$, the total amount feed to the cell, $n_{Ni,f}$, and the amount remaining in the effluent, $n_{Ni,e}$ after 8 h electrodialysis. The difference between the quantity of Ni^{2+} fed to the cell and the quantity transported to the catholyte as well as remaining in the effluent, $n_{Ni,f} - (n_{Ni,k} + n_{Ni,e})$, is also depicted in Figure 3 and is equal to the amount of Ni^{2+} remaining in the bed. After 8 h electrodialysis, the quantity of nickel remaining in the bed is observed to increase substantially with increasing nickel feed concentration. This was primarily due to the formation of a green precipitate, $Ni(OH)_2$ [6], around the outside of the particles at the bottom, or inlet, of the bed; it tended to 'cement' the particles together. The precipitate formed in a triangular region whose sides partially bordered the bottom of the bed and the cation-selective membrane. The green region of precipitation grew in both size and density over time. By comparing the nickel concentration in the effluent with its original concentration in the feed, it was found that an average of 92% of the nickel was removed from the feed solutions.

Typical results for the effluent pH, pH_e, and sodium ion concentration, $n_{Na,e}$, are given in Figure 4 for nickel feed concentrations of 2.8, 4.7 and 5.7×10^{-4} M. For $c_{Ni,f} = 4.7$ and 5.7×10^{-4} M, pH_e increased from approximately 3.5 to 10.3 for a period of time after which it returned to a constant value of approximately 3.1. When $c_{Ni,f} = 2.8 \times 10^{-4}$ M, the pH_e remained nearly constant at 3.5 for the entire experiment; this was also the case for $c_{Ni,f}$ below 2.8×10^{-4} and above 5.7×10^{-4} M. Moreover, the pH_e profile closely followed that of $n_{Na,e}$.

A further experiment was conducted in which a bed of *Amberlyst 15* particles originally in the H^+ form was fed with a 0.001 M $NiSO_4$ solution at a cell voltage of 30 V. Figure 5 depicts the transport of nickel ions from the centre compartment to the cathode compartment during electrodialysis. The amount of Ni^{2+} in the effluent from

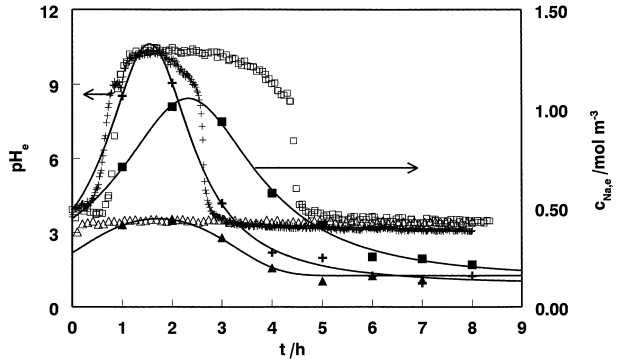

Fig. 4. pH [(△) 2.8×10^{-4}, (□) 4.7×10^{-4}, (+) 5.7×10^{-4} M $NiSO_4$] and sodium content [(▲) 2.8×10^{-4}, (+) 4.7×10^{-4}, (■) 5.7×10^{-4} M $NiSO_4$] of the centre compartment effluent solution with time at various nickel feed concentrations. A constant cell voltage of 30 V was applied across the *Amberlyst 15* ion-exchange bed.

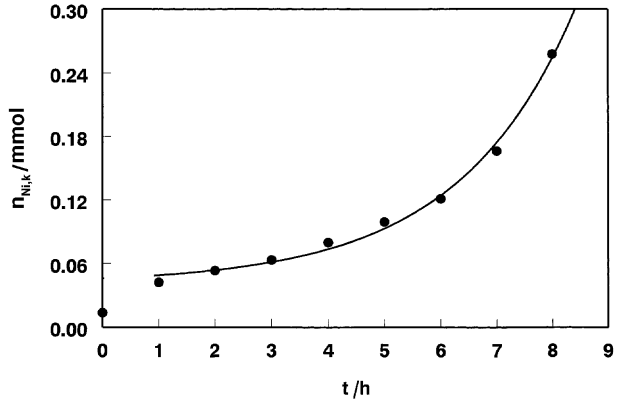

Fig. 5. Nickel content in the catholyte as a function of time for the series of experiments in which a bed of *Amberlyst 15* particles initially in the hydrogen form was used. The nickel concentration and flow rate of the feed solution was 1.0×10^{-3} M and 25 cm^3 min^{-1} respectively. The cell voltage was constant at 30 V.

the centre compartment was less than the detection limit of the AAS instrument (~20 ppb) and after an electrodialysis time of 8 h the quantity of $Ni(OH)_2$ precipitate was significantly less than that observed when *Amberlyst 15* beds originally containing Ni^{2+} and Na^+ were used. The average pH of the effluent was approximately 2.9 during the entire experiment; this is less than that of the previous series using an *Amberlyst 15* bed loaded with Ni^{2+} and Na^+.

A similar experiment was carried out in which a bed of *Dowex 50WX*-2 resin initially in the nickel form was used with a 0.001 M nickel feed. During the experiment it was observed that nickel from the model solution was sorbed nickel or deposited as $Ni(OH)_2$ near the inlet of the cell in the same triangular manner described for *Amberlyst 15*, while the remainder of the bed was regenerated (in contrast to the *Amberlyst 15* resin, a clear distinction between the (green) nickel and (yellow) hydrogen forms of the *Dowex* resin could be observed [2]). Nickel hydroxide formation was only observed in areas of the bed already converted to the nickel form.

3.2. *Current distribution in a tall vertical cell with segmented electrodes*

To determine the current distribution along an ion-exchange bed a cell with segmented electrodes was used. The centre compartment of the cell contained a bed of *Dowex 50WX-2* resin initially in the hydrogen form. A nickel solution was fed upwards through the centre compartment and a cell voltage was applied. The nickel ions were subsequently sorbed by the resin and transported to the cathode compartment under the potential gradient. During the process an interface between the nickel and hydrogen forms of the bed was observed and is termed the nickel front. The position and dispersion of the nickel front were affected by the vertical nickel fluxes produced by feed solution flow and the horizontal fluxes directed towards the cathode compartment produced by the electric potential gradient.

Upon sorption of Ni^{2+} at the front, the ion-exchange particles contracted and caused an increase in the pressure drop of the feed solution through the bed. This produced a decrease in the flow rate of the feed solution that then had to be periodically re-adjusted; more detail of this effect can be found in Ref. [2].

The amount of $Ni(OH)_2$ precipitation was observed to vary with applied cell voltage. No nickel hydroxide was visibly observed to form at a cell voltage of 5 V, but precipitation was observed at cell voltages of 10 and 15 V. It was found on the cathode side of the bed in regions where the ion exchanger had already been converted to the nickel form. The rate at which the nickel front progressed upwards through the column was also observed to decrease with increasing cell voltage.

Figure 6 depicts the current density for various electrode segment pairs at a cell voltage of 5 V as a function of electrodialysis time (the segments increment from 1 at the bottom of the cell where the feed solution

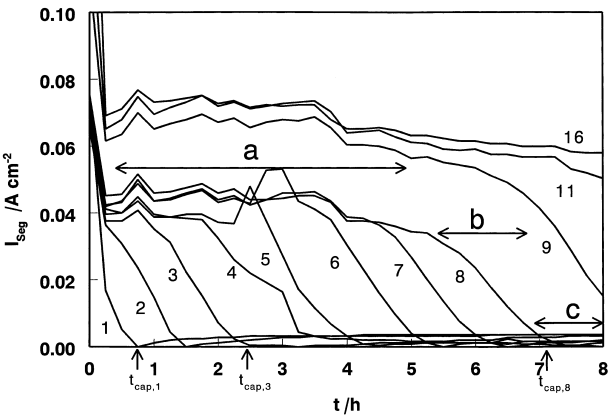

Fig. 6. Current densities across various electrode segment pairs at a 5 V cell voltage vs. electrodialysis time. The ion-exchange compartment contained a bed of *Dowex 50X-2* particles originally in the H^+ form and was fed by a 1.0×10^{-3} M $NiSO_4$ solution at a flow rate of 33 cm^3 min^{-1}. The segments are numerically labelled, where segment 1 is located at the feed inlet of the cell.

was introduced to 20 at the top of the cell). At the start of electrodialysis a relatively high current density through each segment is visible. This was caused by the relatively high interstitial solution conductivity resulting from H_2SO_4 diffusion from the outer compartments before electrodialysis and feed flow was initiated. After the model solution was fed through the centre compartment for approximately 15 min, the conductivity of the centre compartment decreased to a constant level. After this start-up period, the current density across each segment (excepting pairs 1 and 2) was relatively high for a period of time, i.e. 0.04–0.068 A cm^{-2}, and then decreased sequentially along the length of the cell to nearly 0. The current decrease occurred as nickel ions from solution replaced H^+ originally sorbed by the ion exchange particles. Due to the relatively low mobility of sorbed nickel ions, the ion exchange bed increased in resistance upon conversion to the nickel form (the conductivity of the hydrogen and nickel forms of the *Dowex 50W-X2* resin are 6.7 and 2.04×10^{-3} Ω^{-1} cm^{-1} respectively).

After the start-up period, the curves can be divided into three sections; a, b and c, which are depicted in Figure 6 for segment pair 8. Section a, where the current density is relatively large, corresponds to the time during which only H^+ was transported through the bed between segment 8; b, where the current decreases sharply, corresponds to the time period during which Ni^{2+}/H^+ exchange had occurred; and c, where the current density is relatively small, corresponds to the time period during which the bed was largely in the nickel form and only Ni^{2+} was transported across the segment. The location of the nickel front can then be ascertained as a function of electrodialysis time. For instance, the time at which the bed adjacent to an electrode segment was fully converted to the Ni^{2+} form corresponds to the time at which the current across that bed segment reached its lowest level, t_{cap}. In Figure 6, t_{cap} is indicated for three electrode segments.

In Figure 7, the quantity of sorbed nickel, $\bar{n}_{Ni}$, is represented as a function of electrodialysis time, t, for cell voltages of 5, 10 and 15 V. To calculate $\bar{n}_{Ni}$, the volume of the bed in the nickel form, V_{Ni}, was used along with the nickel capacity of the bed, $\bar{c}_{Ni,cap}$, determined in Section 2.3:

$$\bar{n}_{Ni} = \bar{c}_{Ni,cap} V_{Ni} \quad (1)$$

V_{Ni} was calculated as a function of time using the position, or height, of the fixed segment at time t_{cap}:

$$V_{Ni} = z_{t_{cap}} A_b \quad (2)$$

where A_b is the cross-sectional area of the bed perpendicular to the flow of the feed solution.

The quantity of sorbed nickel was observed to decrease with increasing cell voltage. It was clearly larger for a cell voltage of 5 V.

The quantities mentioned above are part of the mass balance of the system:

$$n_{Ni,f} = n_{Ni,k} + \bar{n}_{Ni} + n_{Ni(OH)_2} + n_{Ni,e} + n_{Ni,d} \quad (3)$$

This states that the quantity of nickel introduced to the system, $n_{Ni,f}$, is equal to the sum of the quantity in the catholyte, the quantity sorbed by the resin, the quantity precipitated as $Ni(OH)_2$, the quantity remaining in the effluent and the quantity deposited on the cathode. $n_{Ni,f}$, $n_{Ni,k}$ and $n_{Ni,e}$ were determined by analysing samples using AAS while $\bar{n}_{Ni}$ and $n_{Ni(OH)_2}$ were calculated using Equations (1)–(3). The quantity of nickel in the effluent, $n_{Ni,e}$, was found to be less than the detection limit of the AAS analysis in all cases, whereas the quantity deposited on the cathode, $n_{Ni,d}$, was not observed until later in the 5 V experiment. Figure 7 also shows a comparison between the quantity of Ni^{2+} fed to the cell, $n_{Ni,f}$, with the sum of the quantity sorbed by the bed and transported to the cathode compartment, $(n_{Ni,k} + \bar{n}_{Ni})$, for the 5 V experiment. A good agreement between $n_{Ni,f}$ and $(n_{Ni,k} + \bar{n}_{Ni})$ was found in the 5 V case, but not when cell voltages of 10 and 15 V were used.

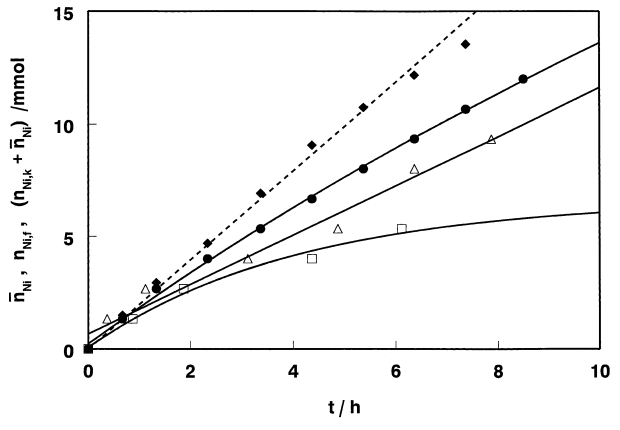

Fig. 7. The quantity of nickel sorbed by the ion exchange bed, $\bar{n}_{Ni}$ [(●) 5; (△) 10; (□) 15 V], and the quantity of nickel fed to the cell, $n_{Ni,f}$ (- - -), are presented as a function of time for the experiments utilising the segmented electrode cell. $n_{Ni,k} + \bar{n}_{Ni}$ is presented for the 5 V experiment (◆). The ion-exchange compartment contained a bed of *Dowex 50X-2* particles originally in the H^+ form and was fed by a 1.0×10^{-3} M $NiSO_4$ solution at a flow rate of 33 cm^3 min^{-1}.

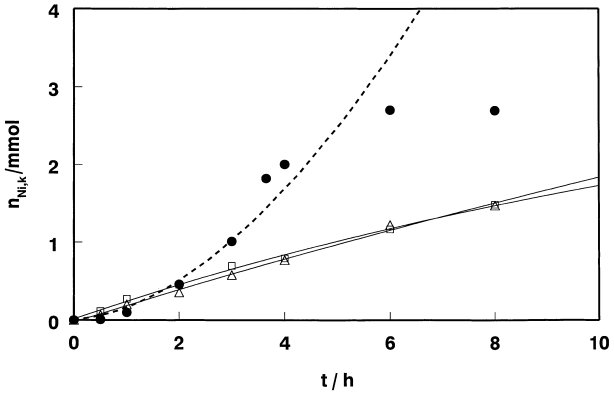

Fig. 8. The quantity of nickel transported to the catholyte, $n_{Ni,k}$ [(●) 5; (△) 10; (□) 15 V] as a function of time. The ion-exchange compartment contained a bed of *Dowex 50X-2* particles initially in the H^+ form and was fed by a 1.0×10^{-3} M $NiSO_4$ solution at a flow rate of 33 cm^3 min^{-1}. The dotted line represents the calculated quantity of nickel transported to the catholyte [Equations (6)–(10)].

The quantity of nickel transported to the catholyte, $n_{Ni,k}$, is given in Figure 8 as a function of time. It was clearly higher for the 5 V experiment (due to the absence of nickel hydroxide formation), but contrary to the 10 and 15 V experiments it was observed to decrease after $t = 5$ h. This was caused by the deposition of metallic nickel on the cathode; such behaviour was also observed in previous work at a cell voltage of 40 V and a nickel concentration in the catholyte of approximately 0.02 mol l^{-1} [2].

4. Discussion

4.1. *Mass transfer during electrodialysis*

4.1.1. *Amberlyst 15*

Nickel ions were removed from the feed solution either by sorption into the ion-exchange particles and subsequent transport to the cathode compartment or by precipitation as $Ni(OH)_2$. For an ion-exchange bed consisting of *Amberlyst 15* resin initially loaded with Ni^{2+} and Na^+ (40 and 60% respectively), it was found that the flux of nickel to the cathode compartment increased with increasing Ni^{2+} feed concentration (Figure 2). This was most likely due to the increased quantity of sorbed Ni^{2+} (note the higher rate of Ni^{2+}/Na^+ exchange exhibited with increasing nickel feed concentration in Figure 4) as well as the increased flux of Ni^{2+} in the solution phase. The majority of nickel removed from the feed solution during the 8 h *Amberlyst 15* experiments, however, remained in the central compartment and its quantity increased practically linearly with nickel feed concentration (Figure 3). One of the consequences of nickel hydroxide precipitation

was a drop in the efficiency of the process. The current efficiency, for example, decreased from an average of approximately 11% after 1 h electrodialysis to approximately 3% after 8 h; there is no clear effect of nickel feed concentration.

Figure 4 indicates that the increase in effluent pH during this series of experiments was related to the exchange of Ni^{2+} in solution with Na^+ in the resin. It shows that after a large part of the sodium ions had been removed from the bed, the effluent pH decreased to a value slightly above 3. The decrease of effluent pH below that of the feed solution ($pH \cong 5.7$) was due to the exchange of Ni^{2+} with sorbed hydrogen and the additional diffusion of sulphuric acid from the outer cell compartments (mainly from the anode compartment [1]). The high effluent pH, i.e. 10.3, during a short period of electrodialysis, was only observed for two experiments in this series and was produced by the formation of NaOH, the mechanism of which was most likely similar to that of $Ni(OH)_2$ formation explained below.

A deposit of nickel hydroxide was found in all *Amberlyst 15* experiments. It was observed to dissolve after electrodialysis and feed flow were stopped as a result of a decrease in the centre compartment pH brought about by sulphuric acid diffusion from the outer compartments. Although dehydrated nickel hydroxide was found to be practically insoluble in 1 M H_2SO_4 [7], the nickel hydroxide formed during this process was most likely hydrated. The dissolution of hydrated $Ni(OH)_2$, which has a solubility product of 6.3×10^{-7} mol^3 m^{-9} [8], occurs at a pH of 3. It follows that the nickel hydroxide was formed in regions of the bed with a pH greater than 3, namely about 7 or higher.

The formation of both $Ni(OH)_2$ and NaOH occurred due to the decomposition of water in the centre compartment. Water dissociation at ion-exchange membranes is well documented [9–14]. 'Extraordinary violent' water dissociation was observed on the desalting surface of a cation exchange membrane placed in a $NiCl_2$ solution [13]. In Ref. [11], the entire current density of 40 mA cm^{-2} across a *Selemion CMV* cation exchange membrane placed in a 0.1 M $NiCl_2$ solution was carried by H^+ formed during $Ni(OH)_2$ precipitation. During electrodialysis, Linkov et al. [6] found nickel hydroxide deposited on particles of cation exchange resin placed in an electrodialysis chamber fed with 0.05 M Na_2SO_4 solutions containing 0.15–0.4 g dm^{-3} Ni^{2+}. To explain the formation of this deposit they proposed that hydrogen and hydroxyl ions were generated on the boundaries of the granules when these were saturated with metal ions. The hydrogen ions were sorbed by the particles to replace nickel ions removed by migration while the hydroxyl ions combined with the nickel to form a hydroxide. Taky et al. [10] proposed that nickel hydroxide precipitation at a cation selective membrane occurred as a result of the decomposition of water molecules involved in the hydration of the nickel ion. These water molecules have a larger equilibrium constant, K_a, than water molecules not complexed with nickel, and should therefore dissociate with greater ease. Based on the work mentioned above, it can be concluded that the dissociation of water, and the consequent precipitation of $Ni(OH)_2$, occurs primarily above the limiting current density for nickel transport. The reactions are as follows [15]:

1. $\left[Ni(H_2O)_6\right]^{2+} \rightarrow \left[NiOH(H_2O)_5\right]^{+} + H^+$
   $K_1 = 5.0 \times 10^{-9}$

2. $\left[NiOH(H_2O)_5\right]^{+} \rightarrow \left[Ni(OH)_2(H_2O)_4\right] + H^+$
   $K_2 = 2.7 \times 10^{-5}$–8.5×10^{-3}

4.1.2. *Dowex 50WX-2*

When a 5 V cell voltage was applied across a bed of *Dowex* 2% cross linked resin initially in the H^+ form, no nickel hydroxide was observed to form in the centre compartment. This also follows from Figure 7 where the following mass balance was shown to be true:

$$n_{Ni,f} = n_{Ni,k} + \bar{n}_{Ni} \tag{4}$$

The deviation at later electrodialysis times ($t > 5$ h) is attributed to nickel deposition on the cathode. For cell voltages greater than 5 V, no metallic nickel deposition was observed. The mass balance given by Equation (3) can then be rearranged to determine the amount of nickel hydroxide formation:

$$n_{Ni(OH)_2} = n_{Ni,f} - \left(n_{Ni,k} + \bar{n}_{Ni}\right) \tag{5}$$

Using Equation 5, the nickel hydroxide precipitation was found to start after 1.11 and 0.43 h electrodialysis at a cell voltage of 10 and 20 V respectively while the rate of precipitation increased with both electrodialysis time and cell voltage.

4.2. *Current distribution in a tall vertical cell*

The current distribution in the hybrid cell was studied using *Dowex 50WX-2*, and the bed's change in conductivity with time was determined. From this information, the distribution of sorbed nickel ions can be determined as a function of time. Figure 9 shows the position of the 'tip' and 'base' of the nickel front as a function of time. The tip represents the time at which the current across an electrode segment began to decrease (Figure 6) due to the sorption of nickel by the ion-exchange bed located adjacent to it. The 'base' of the nickel front represents the position of the front at t_{cap}. The distance between the two lines in Figure 9 indicates the length of the disperse nickel front along the axis of solution flow.

In a conventional ion-exchange bed the velocity at which a concentration front travels through the ion-exchange column can be described by the following equation [4]:

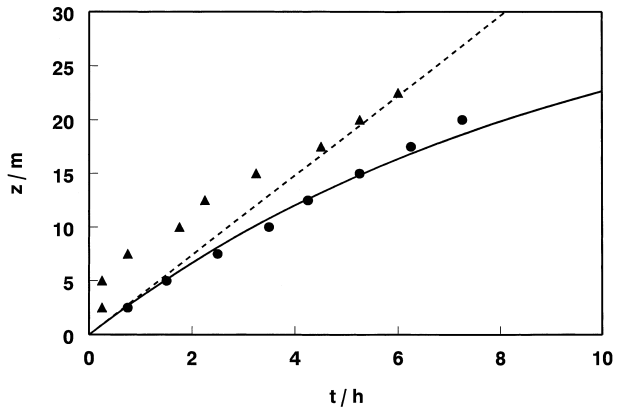

Fig. 9. Height of the tip (▲) and base (●) of the nickel front as a function of time for the 5 V experiment. The ion-exchange compartment contained a bed of *Dowex 50X-2* particles initially in the H^+ form and was fed by a 1.0×10^{-3} M $NiSO_4$ solution at a flow rate of 33 $cm^3\ min^{-1}$. The solid line represents the calculated result [Equations (6)–(9)] while the dotted line represents the height of the nickel front without continuous regeneration of the bed, i.e. conventional ion-exchange.

$$v_F = \frac{\Delta z}{\Delta t} = \frac{v_s}{\frac{\bar{c}_{Ni,cap}}{c_{Ni}} + \varepsilon} \tag{6}$$

where v_F is the velocity of the front in m s^{-1}, v_s the linear solution flow rate in m s^{-1}, $\bar{c}_{Ni,cap}$ the nickel capacity of the resin in mol m^{-3}, c_{Ni} the nickel concentration in the feed solution in mol m^{-3}, ε represents the void fraction of the bed and Δz the distance the nickel front travelled through the bed in time Δt. From this equation the height of the nickel front was calculated as a function of time and is given in Figure 9 as a dotted line. In the hybrid ion-exchange/electrodialysis system described here, however, the change in c_{Ni} due to sorption at continually regenerated sites must first be taken into account. This was done by expressing the mass balance of the system as a function of bed height and then assuming that the rate of sorption in regions of the bed converted to the nickel form was equal to the regeneration rate of the bed, N_{Ni}:

$$c_{Ni} = \frac{Q_s c_{Ni} - wzN_{Ni}}{Q_s,} \tag{7}$$

where c_{Ni} is the concentration of nickel ions in the interstitial solution in regions of the bed completely converted to the nickel form (mol m^{-3}), Q_s the volumetric solution flow rate in $m^3\ s^{-1}$, w the width of the bed perpendicular to the potential gradient in m and N_{Ni} the flux of nickel into the cathode compartment in mol $m^{-2}\ s^{-1}$. By substituting $v_s = 5.5 \times 10^{-3}$ m s^{-1}, $Q_s = 5.5 \times 10^{-7}\ m^3\ s^{-1}$, $c_{Ni,f} = 1.0$ mol m^{-3}, $\bar{c}_{Ni,cap} = 534$ mol m^{-3}, $\varepsilon = 0.5$ and $N_{Ni} = 1.5 \times 10^{-4}$ mol $m^{-2}\ s^{-1}$ into Equations (6) and (7), the height of the bed fully converted to the nickel form was solved as a function of time. N_{Ni} was calculated from the migration term of the Nernst Planck equation:

$$N_{Ni} = z_{Ni}\bar{c}_{Ni,cap}\frac{\bar{D}_{Ni,eff}F}{RT}\text{grad}\,\varphi \tag{8}$$

where $\bar{D}_{Ni,eff}$, the effective diffusion coefficient of nickel in the fully loaded *Dowex 50WX-2* resin, is $1.13 \times 10^{-11}\ m^2\ s^{-1}$ [2]. The potential gradient over the ion-exchange bed is:

$$\text{grad}\,\varphi = \frac{\Delta E_{bed}}{d_{bed}} = \frac{E_{cell} - (E_{anode} + |E_{cathode}| + \Delta E_k + \Delta E_a)}{d_{bed}} = 320\ Vm^{-1} \tag{9}$$

where $(E_{anode} + |E_{cathode}| + \Delta E_k + \Delta E_a)$ was found to be 1.8 V from I/E measurements of the hybrid cell containing the *Dowex* resin. The resistance of the membranes were neglected due their relatively small contribution to the resistance of the cell at low current densities [1]. The calculated height of the 'ideal' nickel front as a function of time is given in Figure 9 as a solid line and it agrees well with the experimental data for the 'base' of the nickel front. The 'tip' of the front cannot be accurately predicted by this model since its formation has largely to do with the migration of ions in the solution phase towards the cathode (the shape of the front is triangular with the hypotenuse running upwards from the anode to the cathode membrane).

This model was further used to simulate the quantity of nickel transported to the catholyte, where:

$$\Delta n_{Ni,k} = (wzN_{Ni})\Delta t, \tag{10}$$

where z is calculated using Equations (6) and (7) as a function of time. The dashed line in Figure 8 shows the calculated result for the 5 V experiment. The agreement between the experimental and calculated result is good until metallic nickel deposition on the cathode occurred. Note that in the above model, the transport of nickel through the solution phase was not taken into consideration and yet the calculated results show a good agreement with the experimental results.

The conductivity of the interstitial solution was lower than that of the ion-exchange particles themselves (4.5×10^{-4} vs. $2.04 \times 10^{-3}\ \Omega^{-1}\ cm^{-1}$) and hence the current during the electrodialysis process flowed mainly through the ion-exchange particles. The three mechanisms of transport include: solely through the resin (R), solely through the solution (S) and alternating through the resin and solution (S–R). The resistance of the ion-exchange bed can then be expressed as [4]:

$$\frac{1}{R_{bed}} = \frac{1}{R_S} + \frac{1}{R_R} + \frac{1}{R_{S-R}} \tag{11}$$

The amount of current transported through the solution phase can be estimated using ohm's law and was found to be 1.4 mA cm^{-2} at a potential gradient over the ion-exchange compartment of 3.2 V cm^{-1}; this compared to an estimated 6.5 mA cm^{-2} through the resin phase. This, along with the agreement between the model and

experimental results, indicate that transport through the resin phase was the predominant transport mechanism of the nickel ions.

The limiting current density to the membrane through the solution phase was estimated by assuming that the transport of ions to the membrane surface was similar to the transport of ions to particle surfaces in a packed bed; the corresponding Sherwood correlation for a packed bed of particles is [16]:

$$Sh = 1.52\,Re^{0.55}Sc^{0.33} \tag{12}$$

where $Re = \frac{vl}{\upsilon}$, $Sc = \frac{\upsilon}{D}$ and l is the characteristic length, in this case the average particle diameter $= 2.25 \times 10^{-4}$ m. Substituting the linear flow rate $v = 5.5 \times 10^{-3}$ m s^{-1}, the kinetic viscosity of water $\upsilon = 8.98 \times 10^{-7}$ m^2 s^{-1} and the diffusion coefficient of Ni^{2+} in water $= 6.9 \times 10^{-10}$ m^2 s^{-1} at 25 °C and very low concentrations [17], into the above equations, the Reynolds, Schmidt and Sherwood numbers were found to be, 1.37, 1301 and 19.33 respectively. The mass transport coefficient, k_m, to the membrane can then be calculated using:

$$Sh = \frac{k_m l}{D_{Ni}} \tag{13}$$

and was found to have a value of 5.93×10^{-5} m s^{-1}. Taking migration into account, the limiting current density to the membrane through the solution phase can be calculated using the following equation [18]:

$$i_{lim} = z_{Ni}\left(1 + \left|\frac{z_{Ni}}{z_{SO_4}}\right|\right)Fkc_{Ni} \tag{14}$$

and was found to be 2.2 mA cm^{-2}. This limiting current density, above which nickel hydroxide precipitation is expected to occur, is greater than the estimated current density transported through the solution phase at a bed voltage of 3.2 V cm^{-1}, i.e. 1.4 mA cm^{-2}. At a bed voltage of 8.2 V cm^{-1} (the 10 V experiment), however, Ohm's law estimates a current density of 3.7 mA cm^{-2}. This is above the calculated limiting current density, which would explain the nickel hydroxide formation at this, and higher, cell voltages.

5. Conclusions

The removal of nickel ions from solution using a combined ion-exchange/electrodialysis technique was studied. The nickel ions were removed by the following mechanisms: either by transport through the solution phase to the cathode compartment, by sorption in the ion-exchanger and subsequent transport to the cathode compartment or by precipitation as a hydroxide in the centre compartment. As the aim of this research program is to create a continuous system for removing nickel ions from very dilute solutions, the latter mechanism must be avoided. Key factors involved in obtaining a continuous system are cell voltage, concentration of nickel in the feed solution and the ionic nature of the ion exchanger. It was shown that the concentration of nickel in the feed affected the quantity of nickel hydroxide in the ion-exchange bed and that the pH of the effluent can be affected by the presence of sodium ions in the resin. Both nickel hydroxide and sodium hydroxide were formed due to the decomposition of water within the central compartment.

The flexible *Dowex 50WX-2* resin performed remarkably better than the macro-reticular *Amberlyst 15* resin; this due to the greater conductivity of the *Dowex* resin. The absence of precipitation in one of the experiments using the *Dowex* 2% cross linked resin showed that it was possible to continuously deionise a dilute nickel solution. Of the cell voltages used, the 1 mM $NiSO_4$ solution in question was deionised without hydroxide precipitation at a cell voltage of 5 V while cell voltages of 10 and 15 and 30 V were high enough to cause $Ni(OH)_2$ formation. The potential gradient over the bed must be chosen sufficiently low. The concentration of nickel and hydrogen ions in the feed solution will also determine whether hydroxide formation will occur and it has been found that the rate of nickel hydroxide precipitation increased with both nickel concentration in the feed as well as cell voltage. Under our experimental conditions, cell voltages higher than about 5 V should be avoided; this corresponds to approximately 320 V m^{-1} bed width.

In previous work it was shown that the current efficiency of the system is 100% when the bed is completely in the nickel form [2]; it follows that the current efficiency of the system greatly depends on the ionic state of the bed. The simple model presented in this paper gives an accurate prediction of the portion of the bed fully converted to the nickel form, where the current efficiency is highest, but it cannot predict the dispersion of the nickel front, where the current efficiency will decrease substantially due to the presence of sorbed hydrogen ions. This model also successfully predicted the quantity of nickel transported to the catholyte as a function of time.

Acknowledgement

The authors are thankful to SENTER (IOP # IZW 97409) for their financial support.

References

1. P.B. Spoor, W.R. ter Veen and L.J.J. Janssen, *J. App. Electrochem.* **31** (2001) 523.
2. P.B. Spoor, W.R. ter Veen and L.J.J. Janssen, *J. Appl. Electrochem.* **31** (2001) 1071.
3. P.B. Spoor, L. Koene, W.R. ter Veen and L.J.J. Janssen, *Chem. Eng. J.* (in press).
4. F. Helfferich, *Ion Exchange* (Dover, New York, 1995).
5. M.P.M.G. Weijs, L.J.J. Janssen and G.J. Visser, *J. Appl. Electrochem.* **27** (1997) 371.

6. N.A. Linkov, J.J. Smit, V.M. Linkov and V.D. Grebenyuk, *J. Appl. Electrochem.* **28** (1998) 1189.
7. K.N. Njau, PhD Thesis, Electrochemical Treatment of Dilute Process Water from a Galvanic Plant, Eindhoven (1998).
8. K.M. Yin, H. Wei, R. Fu, B.N. Popov, S.N. Popov and R.E. White, *J. Appl. Electrochem.* **25** (1995) 543.
9. J.J. Krol, M. Wessling and H. Strathmann, *J. Membrane Sci.* **162** (1999) 145.
10. M. Taky, G. Pourcelly, F. Lebon and C. Gavach, *J. Electroanal. Chem.* **336** (1992) 171.
11. M. Tacky, A. Elmidaoui, G. Pourcelly and C. Gavach, *J. Chim. Phys.* **93** (1996) 386.
12. R. Simons, *Desalination* **28** (1979) 41.
13. Y. Tanaka and M. Seno, *J. Chem. Soc. Faraday Trans. I* **82** (1986) 2065.
14. M. Taky, G. Pourcelly and C. Gavach, *J. Electroanal. Chem.* **336** (1992) 195.
15. A.J. Bard, R. Parsons and J. Jordan, *Standard Potentials in Aqueous Solution* (IUPAC, Marcel Dekker Inc., New York and Basel, 1985).
16. D. Pletcher and F.C. Walsh, *Industrial Electrochemistry* (Blackie Academic & Professional, Glasgow, 1993).
17. R. Parsons, *Handbook of electrochemical constants* (Butterworths Scientific Publications, London, 1959).
18. K.J. Vetter, *Elekrochemishe Kinetik* (Springer-Verlag, Berlin, 1961).